

New Supernova Constraints on Neutrinophilic Dark Sector

Christopher V. Cappiello,^{1,*} P. S. Bhupal Dev,^{1,†} and Amol V. Patwardhan^{2,3,‡}

¹*Department of Physics and McDonnell Center for the Space Sciences,
Washington University, St. Louis, MO 63130, USA*

²*Department of Physics, New York Institute of Technology, New York, NY 10023, USA*

³*School of Physics and Astronomy, University of Minnesota, Minneapolis, MN 55455, USA*

Supernova cooling has long been used to constrain physics beyond the Standard Model, typically involving new mediators or dark matter (DM) particles that couple to nucleons or electrons. In this work, we show that the large density of neutrinos inside the neutrinosphere of supernovae also makes them powerful laboratories to study nonstandard neutrino interactions with a *neutrinophilic* dark sector, i.e. DM and mediator particles interacting primarily with neutrinos. In this case, we find that the existing constraints are rather weak, and for a wide range of currently unconstrained parameter space, neutrino annihilation within a supernova could copiously produce such neutrinophilic DM at a large enough rate to cause noticeable anomalous cooling. From the non-observation of such anomalous cooling in SN1987A, we thus set new constraints on neutrino-DM interactions, which provide up to four orders of magnitude improvement over the existing constraints for DM masses below $\mathcal{O}(100 \text{ MeV})$.

I. INTRODUCTION

The idea that dark matter (DM) or other exotic particles could be constrained by the observation of core-collapse supernova (CCSN) neutrinos was pointed out [1–3] almost as soon as SN 1987A was detected [4–6]. If there exist weakly interacting beyond-Standard-Model (BSM) particles, they could be produced in the dense protoneutron star (PNS) and free-stream out of the supernova, altering its thermal evolution and thus affecting the observed neutrino burst. Supernova cooling has since been used to constrain a multitude of BSM particles, including DM candidates, new force carriers, and Kaluza-Klein modes in extradimensional theories [7, 8]. Due to the enormous neutrino densities within supernovae, it is also possible to use them to probe nonstandard physics in the neutrino sector; see e.g. Refs. [9–42].

In this work, we combine these two ideas, viz., show that neutrino annihilation to DM within a CCSN, followed by the DM free-streaming out of the PNS, could significantly cool the PNS for a wide range of DM masses and couplings. We self-consistently model both the production of DM and its trapping within the neutrinosphere by elastic collisions with neutrinos via a neutrinophilic mediator, in order to compute the extra energy that escapes via the DM from the neutrinosphere. As a result, we get a new stringent constraint on neutrinophilic DM for masses $\lesssim 300 \text{ MeV}$, for a wide range of couplings consistent with thermal production via neutrino annihilation; see Fig. 1. This is different from previous studies which considered DM or mediator production in supernovae using couplings to nucleons/electrons/muons [29, 39, 43–48], where the existing

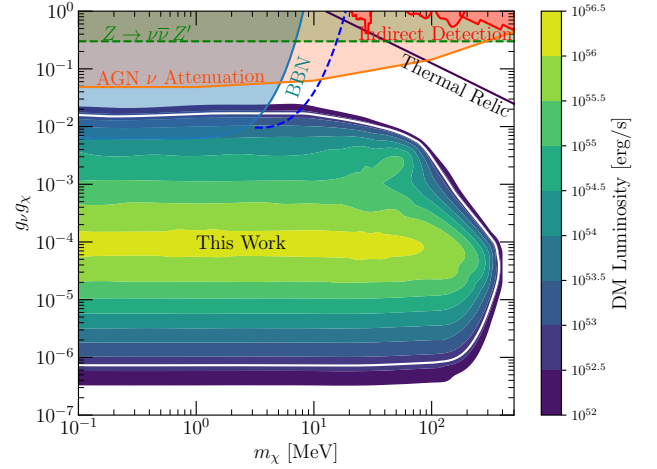


FIG. 1. DM luminosity as a function of the DM mass m_χ and the product of the mediator couplings to neutrinos (g_ν) and DM (g_χ), for a vector mediator mass $m_{Z'} = 10 \text{ GeV}$. The white contour is our SN1987A exclusion limit, set where the emissivity equals $5 \times 10^{52} \text{ erg/s}$. For comparison, we also show exclusion regions from BBN (shaded teal and dashed blue; see text for details), DM indirect detection searches from Super-K data (red) [49, 50], neutrino attenuation in high-energy neutrino sources with DM spikes (orange) [51], and invisible Z decays (dashed green; assumes $g_\nu = g_\chi$) [52, 53]. The black line corresponds to the thermal DM relic density.

laboratory constraints are more stringent than our pure neutrinophilic case.

II. DM-NEUTRINO INTERACTION

For concreteness, we consider a fermionic DM χ which interacts with the SM neutrinos via a massive vector mediator Z' . The relevant part of the interaction La-

* cappiello@wustl.edu

† bdev@wustl.edu

‡ apatwa02@nyit.edu

grangian in the low-energy effective theory is given by

$$-\mathcal{L}_{\text{int}} \supset g_\nu Z'_\mu \bar{\nu} \gamma^\mu P_L \nu + g_\chi Z'_\mu \bar{\chi} \gamma^\mu \chi. \quad (1)$$

For simplicity, we assume that the Z' couplings to all neutrino flavors are equal. Moreover, we take the Z' to be purely neutrinophilic, i.e., it does not couple to the charged leptons or quarks at the leading order, thus evading most of the laboratory constraints. This can arise, for instance, from a gauge-invariant, ultraviolet (UV)-complete model that contains a new heavy fermion charged under an extra $U(1)$ gauge symmetry and mixed with the active neutrinos [54–57]. In this case, loop-induced couplings of Z' to charged leptons and quarks are inevitable [58, 59]; however, their effect is subdominant compared to the effect of the tree-level neutrino coupling for the g_ν values of interest here. Specifically, since the supernova constraint derived here only depends on the product $g_\nu g_\chi$ (cf. Fig. 1) and the dark-sector coupling g_χ by itself is very weakly constrained (from DM self-interaction limit), g_ν can be as small as 10^{-6} and still have a sizable effect on supernova cooling, without any other observable consequence. This makes the supernova constraints derived here a powerful new probe of neutrinophilic dark sector physics, irrespective of the UV-completion details, and complementary to the laboratory searches for neutrinophilic Z' , e.g. via meson decays [52, 58–66], which are only valid for light mediators.

A. Relevant Cross Sections

Given the Lagrangian (1), the DM production inside the supernova happens due to s -channel neutrino-antineutrino annihilation via the Z' mediator, with a cross section

$$\sigma_{\nu_\alpha \bar{\nu}_\alpha \rightarrow \chi \bar{\chi}} = \frac{g_\nu^2 g_\chi^2 (s + 2m_\chi^2)(s + 2m_\nu^2)}{16\pi s [(s - m_{Z'}^2)^2 + m_{Z'}^2 \Gamma_{Z'}^2]} \sqrt{\frac{s - 4m_\chi^2}{s - 4m_\nu^2}}, \quad (2)$$

for each neutrino species ν_α , where s is the squared center-of-momentum (COM) energy, $m_{Z'}$ is the mass of the mediator, m_χ is the mass of the DM, m_ν is the neutrino mass (which can be neglected here, since the neutrinos are relativistic with typical energies of $\mathcal{O}(100 \text{ MeV})$ in the supernova core) and $\Gamma_{Z'}$ is the total decay width of the mediator, given by

$$\Gamma_{Z'} = \frac{g_\nu^2 m_{Z'}}{8\pi} + \frac{g_\chi^2 m_{Z'}}{12\pi} \left(1 + \frac{2m_\chi^2}{m_{Z'}^2} \right) \sqrt{1 - \frac{4m_\chi^2}{m_{Z'}^2}}. \quad (3)$$

Here we have assumed that Z' decay into a DM pair is kinematically allowed, which is always the case in the parameter space we consider.

The same interaction Lagrangian (1) also leads to DM annihilation back into neutrinos, with the corresponding

cross section, summing over all neutrino flavors in the final state, given by

$$\sigma_{\chi \bar{\chi} \rightarrow \nu \bar{\nu}} = \frac{g_\nu^2 g_\chi^2 (s + 2m_\chi^2)(s + 2m_\nu^2)}{12\pi s [(s - m_{Z'}^2)^2 + m_{Z'}^2 \Gamma_{Z'}^2]} \sqrt{\frac{s - 4m_\nu^2}{s - 4m_\chi^2}}, \quad (4)$$

which is same as Eq. (2) with the replacement $\chi \leftrightarrow \nu$, except for an overall factor of $4/3$, accounting for the difference in the total number of initial and final fermion degrees of freedom.

The DM particles, once produced, can also scatter with the ambient neutrinos via the same Z' interaction (1). In the rest frame of the DM, the differential cross section (in terms of the scattering angle θ) is given by

$$\frac{d\sigma_{\nu\chi \rightarrow \nu\chi}}{d\cos\theta} = \frac{g_\nu^2 g_\chi^2}{8\pi} \frac{m_\chi^2 E_\nu^2}{[E_\nu(1 - \cos\theta) + m_\chi]^2} \times \left[\frac{E_\nu^2(\cos\theta - 1)^2 + m_\chi^2(\cos\theta + 1) + E_\nu m_\chi(1 - \cos^2\theta)}{[m_\chi m_{Z'}^2 + E_\nu(1 - \cos\theta)(2E_\nu m_\chi + m_{Z'}^2)]^2} \right]. \quad (5)$$

B. Emissivity Calculation

Assuming spherical symmetry, at a given radial distance r from the center of the supernova core, the rate of neutrino energy going into DM production is given by

$$\dot{E} = \frac{8\pi^2}{(2\pi)^6} \int dE_1 dE_2 d\cos\theta f_1 f_2 E_1^2 E_2^2 (E_1 + E_2) \times \sigma_{\nu\bar{\nu} \rightarrow \chi\bar{\chi}} v_{\text{rel}}, \quad (6)$$

where $v_{\text{rel}} \simeq \sqrt{2(1 - \cos\theta)}$ is the relative velocity between the annihilating neutrino and antineutrino, and the factors $f_{1,2}$ are the Fermi-Dirac distributions of the neutrinos and antineutrinos, given by

$$f_i = \frac{1}{1 + e^{[E_i \pm \mu(r)]/T(r)}}, \quad (7)$$

where the minus (plus) sign corresponds to neutrinos (antineutrinos). In what follows, we suppress the radial dependence, with the understanding that the temperature, chemical potential and density of each neutrino species, are all implicitly functions of the position.

The angular dependence enters the calculation in two ways: through the relative velocity v_{rel} and through the squared COM energy $s = 2E_1 E_2 (1 - \cos\theta)$. Writing the angular dependence explicitly, we perform the angular integral in Eq. (6) analytically and arrive at the emissivity formula

$$\dot{E} = \frac{1}{8\pi^4} \int dE_1 dE_2 f_1 f_2 E_1^2 E_2^2 (E_1 + E_2) \times \frac{g_\nu^2 g_\chi^2}{16\pi [m_{Z'}^4 + m_{Z'}^2 \Gamma_{Z'}^2]} I_c(E_1, E_2, m_\chi), \quad (8)$$

$$\text{where } I_c = \frac{16}{5} (2E_1 E_2 + 3m_\chi^2) \left(1 - \frac{m_\chi^2}{E_1 E_2} \right)^{3/2}.$$

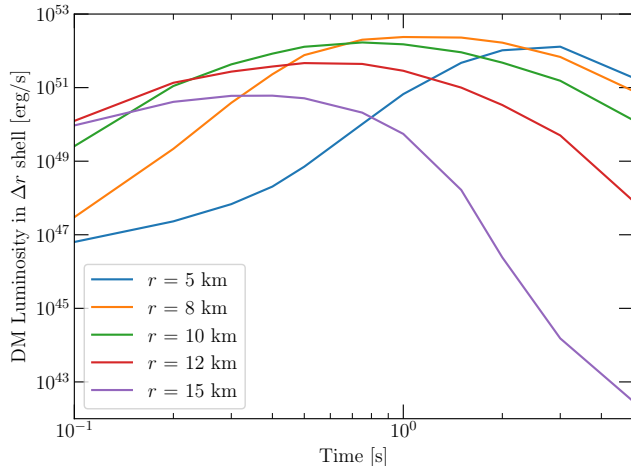


FIG. 2. DM luminosity (i.e. emissivity, multiplied by the volume of a spherical shell with radius Δr), as a function of time at several different radii. Here $m_\chi = 1$ MeV, $m_{Z'} = 10$ GeV, $g_\nu g_\chi = 10^{-6}$, and $\Delta r = 1$ km.

C. Input Parameters

To model the properties of the neutrino population, we use the output of a 1-D CCSN simulation for a $20 M_\odot$ progenitor PNS [67]. This simulation gives profiles of density, temperature and chemical potential both as a function of radius and for several points in time post core bounce. Through the radial dependence of the temperature and chemical potential, \bar{E} is implicitly a function of radius, as will be made explicit below. The details of the simulation and some illustrative plots are given in Appendix A.

Figure 2 shows the amount of neutrino energy going into DM production in several spherical shells as a function of time post bounce. Here the couplings are chosen to be small enough that DM free-streams out of the neutrinosphere without being trapped (see next Section). We see that the highest emission is at about 8 km, and peaks at around 1 second post-bounce. For this reason, we use simulation results for 1 second post-bounce to compute our limits, as this is when the DM emission should be maximized. Note also that 8 km, the radius with the highest emission, is also where the temperature is maximized at 1 second post-bounce (see Appendix A).

D. DM Trapping

It is not enough to merely produce the DM particles: they must also escape from the neutrinosphere. For small enough couplings, virtually all of the DM will escape without scattering. But if the coupling is made large, a DM particle may be trapped, or at least redistribute energy across the neutrinosphere before escaping. Here we restrict ourselves to DM that escapes without scat-

tering.

Because the neutrinos are traveling relativistically, and can be highly degenerate, the mean free path cannot be computed as simply $1/(n_\nu \sigma_{\nu\chi \rightarrow \nu\chi})$, where n_ν is the neutrino number density. First, the neutrino-DM scattering rate is suppressed if the outgoing neutrino energy E_{out} is Pauli-blocked, which is accounted for by the replacement

$$\frac{d\sigma}{dt} \rightarrow [1 - f_i(E_{\text{out}}, \mu, T)] \frac{d\sigma}{dt}, \quad (9)$$

where $t = -2E_\nu^2(1 - \cos\theta)$ is the Mandelstam variable, with E_ν defined in the COM frame. We can thus define a ‘‘Pauli-blocked cross section’’ that takes Pauli-blocking into account:

$$\sigma_{\text{PB}} = \int [1 - f_i(E_{\text{out}}, \mu, T)] \frac{d\sigma}{dt} dt. \quad (10)$$

Second, the fact that the neutrinos are not stationary must be accounted for. In terms of the DM velocity β and the angle between DM and neutrino velocities θ , we can define the relative velocity factor

$$v_{\text{rel}}(E_\chi, \theta) = \sqrt{1 - 2\beta \cos\theta + \beta^2}. \quad (11)$$

With both of these factors accounted for, the scattering rate for a DM particle with neutrinos of species α is

$$\Gamma_i(E_\chi, \theta, \phi) = \frac{n_{\nu_\alpha} v_{\text{rel}}(E_\chi, \theta)}{4\pi[-2T^3 \text{Li}_3(-e^{\mu/T})]} \int dE_\nu E_\nu^2 f(E_\nu) \sigma_{\text{PB}}. \quad (12)$$

Here the factor $-2T^3 \text{Li}_3(x)$, with $\text{Li}_3(x)$ being the polylogarithm function, is a normalization factor to the Fermi-Dirac distribution times density of states, the function which determines the probability of a given neutrino energy.

We thus define the inverse mean free path, reintroducing the explicit position dependence:

$$\lambda^{-1}(E_\chi, \mathbf{r}) = \frac{2\pi}{\beta} \int \sum_i \Gamma_i(E_\chi, \theta, \phi) d\cos\theta. \quad (13)$$

From this, we can compute the probability for a DM particle to escape the neutrinosphere without scattering:

$$P_0(E_\chi) = \exp\left(-\int \frac{ds}{\lambda(E_\chi, \mathbf{r})}\right), \quad (14)$$

where s is the path traveled by the DM, which in general is a function of r , as well as the angular variables θ and ϕ . If we imagine that after being produced at a radius r_0 , all the DM particles travel on radial trajectories directly out of the neutrinosphere, Eq. (14) simplifies to

$$P_0(E_\chi, r_0) = \exp\left(-\int_{r_0}^{\infty} \frac{dr}{\lambda(E_\chi, r)}\right). \quad (15)$$

Although assuming a radial trajectory underestimates the true value of the integral in the exponent for most

DM particles, it is accurate to within a factor of 2 for a substantial fraction of the DM, depending on the value of r_0 . It would also be overly conservative to assume that only particles that escape without scattering can result in cooling: DM particles that scatter once or a couple times could still carry away significant energy. Therefore, we consider the above formula a reasonable estimate of the suppression of the energy emission due to trapping.

We also note that after being produced, DM can also annihilate back into neutrinos inside the neutrinosphere. However, even for the largest DM luminosity that can be produced (which requires $g_\nu g_\chi \simeq 10^{-4}$; see Fig. 1), we checked that the ambient neutrino number density exceeds the produced DM number density by about an order of magnitude. For larger couplings, DM and neutrinos deep inside the neutrinosphere may come into thermal equilibrium. But at those couplings, the DM luminosity is dominated by production at larger radii (see Fig. 3), where the produced DM density is still much lower than the neutrino density. Therefore, we do not include the DM annihilation in the escape probability above.

Using the average DM energy E_{avg} to compute the escape probability, we define the emissivity after trapping is taken into account as

$$\mathcal{E}(r) = P_0(E_{\text{avg}}, r) \dot{E}(r), \quad (16)$$

with \dot{E} given by Eq. (8). In Fig. 3, we show the DM luminosity per spherical shell for a range of different coupling values. For concreteness, we choose a DM mass of 1 MeV and a mediator mass of 10 GeV. When the couplings are small, the luminosity peaks at about 8 km (where the temperature peaks), and increasing the couplings increases the total energy emission. However, when the couplings become large, any DM produced near the center of the neutrinosphere is effectively trapped, and the emission is dominated by larger radii. Integrating these emission profiles over r yields the total luminosity for a given choice of model parameters, namely, couplings and particle masses.

III. RESULTS

Figure 1 shows the total energy loss rate to DM at 1 second post-bounce for a range of model parameters. For concreteness, we set the mediator mass $m_{Z'} = 10$ GeV, and scan over values of DM mass and couplings. As both the emission and trapping depend only on the product $g_\nu g_\chi$, we do not vary the couplings independently, instead scanning over values of their product. For small couplings ($g_\nu g_\chi \lesssim 10^{-6}$), the DM production rate is too small to have a noticeable effect on the supernova. For large couplings ($g_\nu g_\chi \gtrsim 10^{-2}$), the production rate is large, but the DM is trapped effectively enough that very little energy escapes. Such trapped DM could still redistribute energy within the neutrinosphere, potentially leading to more subtle but still detectable signals, but we do not

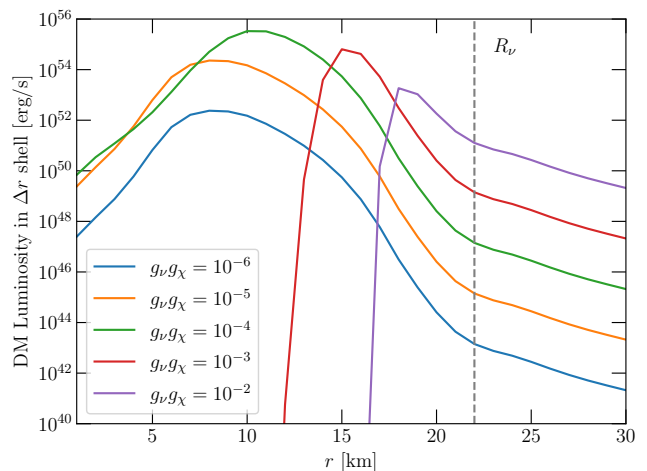


FIG. 3. DM luminosity (including trapping effect) at $t = 1$ s in each 1-km-wide spherical shell as a function of radius. Here $m_\chi = 1$ MeV, and $m_{Z'} = 10$ GeV. Note that the horizontal axis starts at 1 km, because the value on the vertical axis goes to zero at $r = 0$.

consider this effect here, as it requires a detailed supernova simulation which is beyond the scope of this work. At the right edge of the plot, the DM is too heavy to be efficiently produced (note that the typical neutrino energies are $\mathcal{O}(100)$ MeV; see the plots in Appendix A).

In the central, multicolored region of Fig. 1, the DM luminosity may be substantial compared to the neutrino luminosity. The white line denotes a luminosity of 5×10^{52} erg/s, which is approximately 10% of the maximum neutrino luminosity produced by the simulations of Ref. [67]. This also agrees roughly with the ‘‘Raffelt criterion’’ based on observations of SN 1987A, namely that any exotic energy loss should not exceed the neutrino luminosity of 3×10^{52} erg/s [68]. Within this white contour, the DM emission would be substantial enough to alter the evolution of the supernova, and we thus consider the parameter space within this contour to be ruled out. We also see that only slightly within this contour, the emission can be an order of magnitude higher, such that requiring a somewhat larger luminosity of, e.g., 10^{53} erg/s would not substantially change our limit. Similarly, we do not expect the current modeling uncertainties on the CCSN parameters [69] to significantly change our results either, as shown in case of other BSM particles [70, 71].

The black line in the top right corner of Fig. 1 denotes the parameters required for the DM to obtain the correct relic abundance via thermal freeze-out, obtained by setting

$$\langle \sigma_{\chi\bar{\chi} \rightarrow \nu\bar{\nu}} \rangle \simeq \frac{g_\nu^2 g_\chi^2}{2\pi} \frac{m_\chi^2}{(4m_\chi^2 - m_{Z'}^2)^2 + m_{Z'}^2 \Gamma_{Z'}^2} \simeq 3 \times 10^{-26} \text{cm}^3/\text{s}, \quad (17)$$

where we have used Eq. (4) in the non-relativistic limit. Although the parameter space we constrain does not

quite reach the thermal relic line and thus overproduces DM, it effectively constrains various other possibilities of obtaining the correct relic abundance, such as DM annihilation to lighter dark states [72], or entropy injection into the SM plasma following DM decoupling [73].

In Fig. 1, the parameter space in teal is excluded by big bang nucleosynthesis (BBN) considerations. This limit is derived by setting the Hubble rate H equal to the DM production rate [cf. Eq. (6) without the $(E_1 + E_2)$ factor, divided by the neutrino density] at $T = 1$ MeV. Note that the constraint becomes flat at low m_χ because, in this limit, $m_\chi^2 < s$ and $\sigma_{\nu\bar{\nu} \rightarrow \chi\bar{\chi}}$ becomes independent of mass. Another BBN limit can also be set by comparing the rate for the opposite process $\chi\bar{\chi} \rightarrow \nu\bar{\nu}$, i.e. $\Gamma_\chi = n_\chi \langle \sigma_{\chi\bar{\chi} \rightarrow \nu\bar{\nu}} v_\chi \rangle$, to the Hubble rate, because an excess neutrino production could alter the neutron-to-proton ratio at the time of BBN. However, setting such a limit requires an assumed DM density. Although the parameter space we show lies largely below the thermal relic line, for reference we compute the BBN bound that results from a thermal DM density of $n_\chi = g(m_\chi T/2\pi)^{3/2} e^{-m_\chi/T}$ (with $g = 2$ for DM), resulting in the dashed blue curve in Fig. 1, which extends to slightly higher masses. We stop this curve at $m_\chi = 3$ MeV because the formula we use for the DM density assumes that the DM is nonrelativistic.

The pink region is excluded based on the non-observation of attenuation of high energy neutrinos produced in the nearby active galaxy NGC 1068 [74], assuming that it contains a DM spike [51]. There exist additional constraints based on scattering between spiked DM and neutrinos from the blazar TXS 0506+05 [75, 76] and tidal disruption events (TDE) such as AT2019dsg [77], which are weaker than the NGC 1068 bound in the parameter space considered here, and hence, not shown in Fig. 1. Similarly, there exist cosmological constraints from small-scale structure formation and galactic density profiles [78, 79], as well as from Cosmic Microwave Background and large-scale structure [80, 81], which are however weaker for heavy mediators and do not show up in the parameter space of our interest.

There also exist constraints on our parameter space from DM indirect detection limits. We show limits from 3 analyses of Super-K data, two of which were first presented in Ref. [50] and the third is reproduced from Ref. [49], collectively shown as the red-shaded region.

The model we consider also allows for neutrino self-interactions via the Z' mediator. We show the constraint on this interaction arising from invisible Z decays [52, 53]. As this limit is independent of any DM interaction, it does not actually constrain g_χ ; for reference, we plot this bound under the assumption that $g_\chi = g_\nu$. Note that even large neutrino self-interactions have little impact on the supernova dynamics [36, 82], which justifies our use of the standard CCSN simulation results [67] for our purpose.

Our model also allows for DM self interactions, but self interaction bounds from e.g. the Bullet Cluster [83]

are not strong enough to constrain the parameter space shown here.

IV. DISCUSSION AND CONCLUSION

In conclusion, we derived new supernova constraints on neutrinophilic DM which are up to four orders of magnitude stronger than the existing constraints for DM masses below $\mathcal{O}(100)$ MeV. Here, we considered fermion DM and vector mediator for concreteness, but it is straightforward to generalize our work to any combination of DM and mediator type (scalar, pseudo-scalar, fermion, vector and axial-vector).

In this work, we reported limits assuming a mediator mass of 10 GeV. For heavier mediators, our results can easily be rescaled by simply keeping the ratio $g_\nu^2 g_\chi^2 / m_{Z'}^4$ constant. For lighter mediators, the rescaling is less straightforward, due to the resonance at $s = m_{Z'}^2$. Although the typical neutrino energies are of order 100 MeV, even mediators as heavy as 1 GeV can be produced on shell at a high enough rate to noticeably affect the total neutrino annihilation rate; above roughly 2 GeV, the rate becomes negligible. The corresponding increase in the production cross section means that our limits could be much stronger for MeV-scale mediators. However, this would also allow the mediator to be produced on shell and possibly escape before decaying, creating an additional cooling channel and requiring a more detailed treatment of trapping. We defer consideration of this regime to future work.

ACKNOWLEDGMENTS

We would like to thank Hans-Thomas Janka for providing access to simulation data through the Garching Core Collapse Supernova Archive. The particular simulation whose output was used for our work was done by Robert Bollig and Lorenz Hüdepohl using the PROMETHEUS-VERTEX code. In addition, we thank Gonzalo Herrera and Manibrata Sen for useful discussions. B.D. also thanks Doojin Kim, Deepak Sathyan, Kuver Sinha and Yongchao Zhang for ongoing collaboration on a related topic which led to this project, and the organizers of the BCVSPIN 2024 conference in Kathmandu, Nepal, for warm hospitality where part of this work was done. The work of B.D. was partly supported by the US Department of Energy under grant No. DE-SC0017987. C.V.C. was generously supported by the Arthur B. McDonald Canadian Astroparticle Physics Research Institute, and by Washington University in St. Louis through the Edwin Thompson Jaynes Postdoctoral Fellowship. A.V.P. thanks Sanjay Reddy for helpful discussions and acknowledges partial support from the U.S. Department of Energy (DOE) under grant DE-FG02-87ER40328 at the University of Minnesota.

Appendix A: Simulation Inputs

For the calculations presented in this paper, we use the output of a CCSN simulation for a $20 M_{\odot}$ progenitor with the SFHo equation of state and without muons in

the PNS [67]. We take a snapshot of the baryon density ρ , temperature T , electron neutrino chemical potential μ_{ν_e} and number densities of neutrinos and antineutrinos of all flavors as functions of radius r at 1.0 s post core bounce. These profiles are depicted in Fig. 4. This particular snapshot is chosen because it has the maximum overall DM luminosity, see Fig. 2.

-
- [1] J. R. Ellis and K. A. Olive, *Phys. Lett. B* **193**, 525 (1987).
 [2] G. Raffelt and D. Seckel, *Phys. Rev. Lett.* **60**, 1793 (1988).
 [3] M. S. Turner, *Phys. Rev. Lett.* **60**, 1797 (1988).
 [4] K. Hirata *et al.* (Kamiokande-II), *Phys. Rev. Lett.* **58**, 1490 (1987).
 [5] R. M. Bionta *et al.*, *Phys. Rev. Lett.* **58**, 1494 (1987).
 [6] E. N. Alekseev, L. N. Alekseeva, I. V. Krivosheina, and V. I. Volchenko, *Phys. Lett. B* **205**, 209 (1988).
 [7] G. G. Raffelt, *Stars as laboratories for fundamental physics: The astrophysics of neutrinos, axions, and other weakly interacting particles* (1996).
 [8] R. Essig *et al.*, in *Snowmass 2013: Snowmass on the Mississippi* (2013) [arXiv:1311.0029 \[hep-ph\]](#).
 [9] D. A. Dicus, E. W. Kolb, and D. L. Tubbs, *Nucl. Phys. B* **223**, 532 (1983).
 [10] E. W. Kolb and M. S. Turner, *Phys. Rev. D* **36**, 2895 (1987).
 [11] A. Manohar, *Phys. Lett. B* **192**, 217 (1987).
 [12] D. A. Dicus, S. Nussinov, P. B. Pal, and V. L. Teplitz, *Phys. Lett. B* **218**, 84 (1989).
 [13] G. M. Fuller, R. Mayle, and J. R. Wilson, *Astrophys. J.* **332**, 826 (1988).
 [14] K. Kainulainen, J. Maalampi, and J. T. Peltoniemi, *Nucl. Phys. B* **358**, 435 (1991).
 [15] X. Shi and G. Sigl, *Phys. Lett. B* **323**, 360 (1994), [Erratum: *Phys. Lett. B* 324, 516–516 (1994)], [arXiv:hep-ph/9312247](#).
 [16] E. W. Kolb, R. N. Mohapatra, and V. L. Teplitz, *Phys. Rev. Lett.* **77**, 3066 (1996), [arXiv:hep-ph/9605350](#).
 [17] H. Nunokawa, J. T. Peltoniemi, A. Rossi, and J. W. F. Valle, *Phys. Rev. D* **56**, 1704 (1997), [arXiv:hep-ph/9702372](#).
 [18] J. Hidaka and G. M. Fuller, *Phys. Rev. D* **74**, 125015 (2006), [arXiv:astro-ph/0609425](#).
 [19] J. Hidaka and G. M. Fuller, *Phys. Rev. D* **76**, 083516 (2007), [arXiv:0706.3886 \[astro-ph\]](#).
 [20] G. M. Fuller, A. Kusenko, and K. Petraki, *Phys. Lett. B* **670**, 281 (2009), [arXiv:0806.4273 \[astro-ph\]](#).
 [21] M. Blennow, A. Mirizzi, and P. D. Serpico, *Phys. Rev. D* **78**, 113004 (2008), [arXiv:0810.2297 \[hep-ph\]](#).
 [22] C. A. Argüelles, V. Brdar, and J. Kopp, *Phys. Rev. D* **99**, 043012 (2019), [arXiv:1605.00654 \[hep-ph\]](#).
 [23] L. Heurtier and Y. Zhang, *JCAP* **02**, 042 (2017), [arXiv:1609.05882 \[hep-ph\]](#).
 [24] A. Das, A. Dighe, and M. Sen, *JCAP* **05**, 051 (2017), [arXiv:1705.00468 \[hep-ph\]](#).
 [25] A. Dighe and M. Sen, *Phys. Rev. D* **97**, 043011 (2018), [arXiv:1709.06858 \[hep-ph\]](#).
 [26] Y. Yang and J. P. Kneller, *Phys. Rev. D* **97**, 103018 (2018), [arXiv:1803.04504 \[astro-ph.HE\]](#).
 [27] S. Shalgar, I. Tamborra, and M. Bustamante, *Phys. Rev. D* **103**, 123008 (2021), [arXiv:1912.09115 \[astro-ph.HE\]](#).
 [28] A. M. Suliga, I. Tamborra, and M.-R. Wu, *JCAP* **08**, 018 (2020), [arXiv:2004.11389 \[astro-ph.HE\]](#).
 [29] A. M. Suliga and I. Tamborra, *Phys. Rev. D* **103**, 083002 (2021), [arXiv:2010.14545 \[hep-ph\]](#).
 [30] K. Akita, S. H. Im, and M. Masud, *JHEP* **12**, 050 (2022), [arXiv:2206.06852 \[hep-ph\]](#).
 [31] P.-W. Chang, I. Esteban, J. F. Beacom, T. A. Thompson, and C. M. Hirata, *Phys. Rev. Lett.* **131**, 071002 (2023), [arXiv:2206.12426 \[hep-ph\]](#).
 [32] Y.-M. Chen, M. Sen, W. Tangarife, D. Tuckler, and Y. Zhang, *JCAP* **11**, 014 (2022), [arXiv:2207.14300 \[hep-ph\]](#).
 [33] D. F. G. Fiorillo, G. G. Raffelt, and E. Vitagliano, *Phys. Rev. Lett.* **131**, 021001 (2023), [arXiv:2209.11773 \[hep-ph\]](#).
 [34] C. A. Manzari, J. Martin Camalich, J. Spinner, and R. Ziegler, *Phys. Rev. D* **108**, 103020 (2023), [arXiv:2307.03143 \[hep-ph\]](#).
 [35] A. Ray and Y.-Z. Qian, *Phys. Rev. D* **108**, 063025 (2023), [arXiv:2306.08209 \[hep-ph\]](#).
 [36] D. F. G. Fiorillo, G. G. Raffelt, and E. Vitagliano, *Phys. Rev. Lett.* **132**, 021002 (2024), [arXiv:2307.15115 \[hep-ph\]](#).
 [37] G. Chauhan, S. Horiuchi, P. Huber, and I. M. Shoemaker, (2023), [arXiv:2309.05860 \[hep-ph\]](#).
 [38] P. Carezza, G. Lucente, L. Mastrototaro, A. Mirizzi, and P. D. Serpico, *Phys. Rev. D* **109**, 063010 (2024), [arXiv:2311.00033 \[hep-ph\]](#).
 [39] K.-C. Lai, C. S. J. Leung, and G.-L. Lin, *Phys. Rev. D* **110**, 103023 (2024), [arXiv:2401.16023 \[hep-ph\]](#).
 [40] A. Ray and Y.-Z. Qian, *Phys. Rev. D* **110**, 043007 (2024), [arXiv:2404.14485 \[hep-ph\]](#).
 [41] B. Telalovic, D. F. G. Fiorillo, P. Martínez-Miravé, E. Vitagliano, and M. Bustamante, *JCAP* **11**, 011 (2024), [arXiv:2406.15506 \[hep-ph\]](#).
 [42] A. M. Suliga, P. C.-K. Cheong, J. Froustey, G. M. Fuller, L. Gráf, K. Kehrer, O. Scholer, and S. Shalgar, (2024), [arXiv:2410.01080 \[hep-ph\]](#).
 [43] P. Fayet, D. Hooper, and G. Sigl, *Phys. Rev. Lett.* **96**, 211302 (2006), [arXiv:hep-ph/0602169](#).
 [44] W. DeRocco, P. W. Graham, D. Kasen, G. Marques-Tavares, and S. Rajendran, *Phys. Rev. D* **100**, 075018 (2019), [arXiv:1905.09284 \[hep-ph\]](#).
 [45] D. Croon, G. Elor, R. K. Leane, and S. D. McDermott, *JHEP* **01**, 107 (2021), [arXiv:2006.13942 \[hep-ph\]](#).
 [46] A. Sung, G. Guo, and M.-R. Wu, *Phys. Rev. D* **103**, 103005 (2021), [arXiv:2102.04601 \[hep-ph\]](#).
 [47] A. Caputo, G. Raffelt, and E. Vitagliano, *Phys. Rev. D* **105**, 035022 (2022), [arXiv:2109.03244 \[hep-ph\]](#).

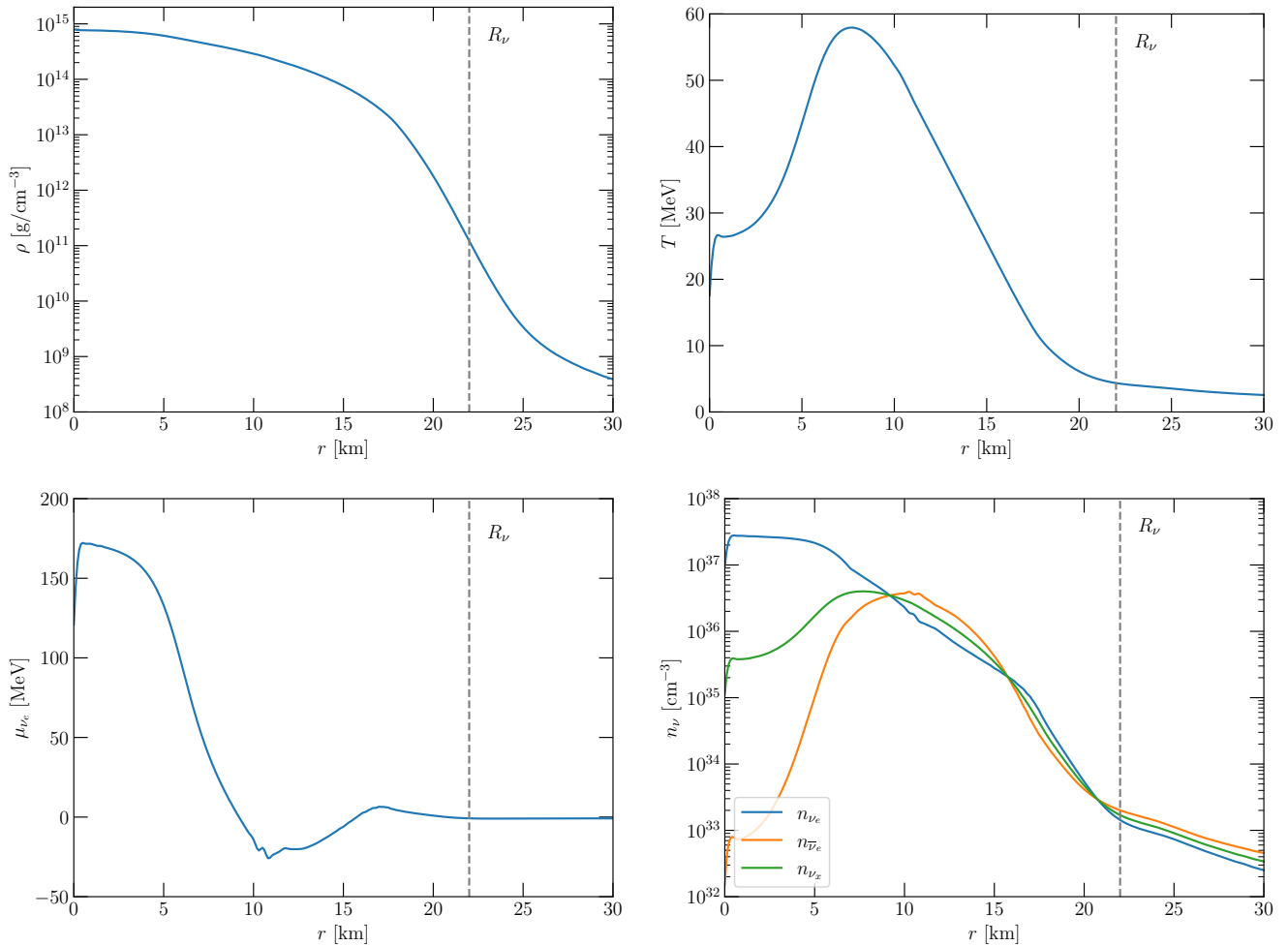


FIG. 4. Profiles of baryon density ρ , temperature T , electron neutrino chemical potential μ_{ν_e} and number densities of neutrinos and antineutrinos at 1.0 s post core bounce in a CCSN simulation with a $20 M_\odot$ progenitor and standard physics. The vertical dashed lines indicate the position of the neutrino sphere (R_ν).

- [48] D. G. Cerdeño, M. Cermeño, and Y. Farzan, *Phys. Rev. D* **107**, 123012 (2023), arXiv:2301.00661 [hep-ph].
- [49] A. Olivares-Del Campo, C. Bøehm, S. Palomares-Ruiz, and S. Pascoli, *Phys. Rev. D* **97**, 075039 (2018), arXiv:1711.05283 [hep-ph].
- [50] C. A. Argüelles, A. Diaz, A. Kheirandish, A. Olivares-Del-Campo, I. Safa, and A. C. Vincent, *Rev. Mod. Phys.* **93**, 035007 (2021), arXiv:1912.09486 [hep-ph].
- [51] J. M. Cline and M. Puel, *JCAP* **06**, 004 (2023), arXiv:2301.08756 [hep-ph].
- [52] R. Laha, B. Dasgupta, and J. F. Beacom, *Phys. Rev. D* **89**, 093025 (2014), arXiv:1304.3460 [hep-ph].
- [53] P. S. B. Dev, D. Kim, D. Sathyan, K. Sinha, and Y. Zhang, (2024), arXiv:2407.12738 [hep-ph].
- [54] J. F. Cherry, A. Friedland, and I. M. Shoemaker, (2014), arXiv:1411.1071 [hep-ph].
- [55] Y. Farzan and J. Heeck, *Phys. Rev. D* **94**, 053010 (2016), arXiv:1607.07616 [hep-ph].
- [56] Y. Farzan and M. Tortola, *Front. in Phys.* **6**, 10 (2018), arXiv:1710.09360 [hep-ph].
- [57] W. Abdallah, A. K. Barik, S. K. Rai, and T. Samui, *Phys. Rev. D* **104**, 095031 (2021), arXiv:2106.01362 [hep-ph].
- [58] G. Chauhan and X.-J. Xu, *JHEP* **04**, 003 (2021), arXiv:2012.09980 [hep-ph].
- [59] G. Chauhan, P. S. B. Dev, and X.-J. Xu, *Phys. Lett. B* **841**, 137907 (2023), arXiv:2204.11876 [hep-ph].
- [60] P. Bakhti and Y. Farzan, *Phys. Rev. D* **95**, 095008 (2017), arXiv:1702.04187 [hep-ph].
- [61] P. Bakhti, Y. Farzan, and M. Rajaei, *Phys. Rev. D* **99**, 055019 (2019), arXiv:1810.04441 [hep-ph].
- [62] G. Arcadi, J. Heeck, F. Heizmann, S. Mertens, F. S. Queiroz, W. Rodejohann, M. Slezák, and K. Valerius, *JHEP* **01**, 206 (2019), arXiv:1811.03530 [hep-ph].
- [63] M. Bahrminasr, P. Bakhti, and M. Rajaei, *J. Phys. G* **48**, 095001 (2021), arXiv:2003.09985 [hep-ph].
- [64] P. Bakhti, M. Rajaei, and S. Shin, *Phys. Rev. D* **109**, 095043 (2024), arXiv:2311.14945 [hep-ph].
- [65] P. S. B. Dev, B. Dutta, T. Han, and D. Kim, *Phys. Lett. B* **850**, 138500 (2024), arXiv:2304.02031 [hep-ph].

- [66] W. Bai, J. Liao, and H. Liu, *Phys. Rev. D* **110**, 115031 (2024), [arXiv:2409.01826 \[hep-ph\]](#).
- [67] H.-T. Janka, “The garching core-collapse supernova archive,” .
- [68] G. G. Raffelt, *Phys. Rept.* **198**, 1 (1990).
- [69] H. T. Janka, (2025), [arXiv:2502.14836 \[astro-ph.HE\]](#).
- [70] J. H. Chang, R. Essig, and S. D. McDermott, *JHEP* **09**, 051 (2018), [arXiv:1803.00993 \[hep-ph\]](#).
- [71] S. Balaji, P. S. B. Dev, J. Silk, and Y. Zhang, *JCAP* **12**, 024 (2022), [arXiv:2205.01669 \[hep-ph\]](#).
- [72] P. N. Bhattiprolu, R. McGehee, and A. Pierce, *Phys. Rev. D* **110**, L031702 (2024), [arXiv:2312.14152 \[hep-ph\]](#).
- [73] J. A. Evans, A. Ghalsasi, S. Gori, M. Tammaro, and J. Zupan, *JHEP* **02**, 151 (2020), [arXiv:1910.06319 \[hep-ph\]](#).
- [74] R. Abbasi *et al.* (IceCube), *Science* **378**, 538 (2022), [arXiv:2211.09972 \[astro-ph.HE\]](#).
- [75] J. M. Cline, S. Gao, F. Guo, Z. Lin, S. Liu, M. Puel, P. Todd, and T. Xiao, *Phys. Rev. Lett.* **130**, 091402 (2023), [arXiv:2209.02713 \[hep-ph\]](#).
- [76] F. Ferrer, G. Herrera, and A. Ibarra, *JCAP* **05**, 057 (2023), [arXiv:2209.06339 \[hep-ph\]](#).
- [77] M. Fujiwara and G. Herrera, *Phys. Lett. B* **851**, 138573 (2024), [arXiv:2312.11670 \[hep-ph\]](#).
- [78] K. Akita and S. Ando, *JCAP* **11**, 037 (2023), [arXiv:2305.01913 \[astro-ph.CO\]](#).
- [79] S. Heston, S. Horiuchi, and S. Shirai, *Phys. Rev. D* **110**, 023004 (2024), [arXiv:2402.08718 \[hep-ph\]](#).
- [80] G. Mangano, A. Melchiorri, P. Serra, A. Cooray, and M. Kamionkowski, *Phys. Rev. D* **74**, 043517 (2006), [arXiv:astro-ph/0606190](#).
- [81] R. J. Wilkinson, C. Boehm, and J. Lesgourgues, *JCAP* **05**, 011 (2014), [arXiv:1401.7597 \[astro-ph.CO\]](#).
- [82] D. F. G. Fiorillo, G. G. Raffelt, and E. Vitagliano, *Phys. Rev. D* **109**, 023017 (2024), [arXiv:2307.15122 \[hep-ph\]](#).
- [83] M. Markevitch, A. H. Gonzalez, D. Clowe, A. Vikhlinin, L. David, W. Forman, C. Jones, S. Murray, and W. Tucker, *Astrophys. J.* **606**, 819 (2004), [arXiv:astro-ph/0309303](#).